Interplay of the Norrin and Wnt7a/Wnt7b signaling systems in blood–brain barrier and blood–retina barrier development and maintenance

Yanshu Wang[a,b], Chris Cho[a], John Williams[a,b], Philip M. Smallwood[a,b], Chi Zhang[c], Harald J. Junge[c], and Jeremy Nathans[a,b,d,e,1]

[a]Department of Molecular Biology and Genetics, The Johns Hopkins University School of Medicine, Baltimore, MD 21205; [b]Howard Hughes Medical Institute, The Johns Hopkins University School of Medicine, Baltimore, MD 21205; [c]Department of Molecular, Cellular, and Developmental Biology, University of Colorado, Boulder, CO 80309; [d]Department of Neuroscience, The Johns Hopkins University School of Medicine, Baltimore, MD 21205; and [e]Department of Ophthalmology, The Johns Hopkins University School of Medicine, Baltimore, MD 21205

Contributed by Jeremy Nathans, October 23, 2018 (sent for review August 2, 2018; reviewed by Chenghua Gu and Brad St. Croix)

β-Catenin signaling controls the development and maintenance of the blood–brain barrier (BBB) and the blood–retina barrier (BRB), but the division of labor and degree of redundancy between the two principal ligand–receptor systems—the Norrin and Wnt7a/Wnt7b systems—are incompletely defined. Here, we present a loss-of-function genetic analysis of postnatal BBB and BRB maintenance in mice that shows striking threshold and partial redundancy effects. In particular, the combined loss of Wnt7a and Norrin or Wnt7a and Frizzled4 (Fz4) leads to anatomically localized BBB defects that are far more severe than observed with loss of Wnt7a, Norrin, or Fz4 alone. In the cerebellum, selective loss of Wnt7a in glia combined with ubiquitous loss of Norrin recapitulates the phenotype observed with ubiquitous loss of both Wnt7a and Norrin, implying that glia are the source of Wnt7a in the cerebellum. Tspan12, a coactivator of Norrin signaling in the retina, is also active in BBB maintenance but is less potent than Norrin, consistent with a model in which Tspan12 enhances the amplitude of the Norrin signal in vascular endothelial cells. Finally, in the context of a partially impaired Norrin system, the retina reveals a small contribution to BRB development from the Wnt7a/Wnt7b system. Taken together, these experiments define the extent of CNS region-specific cooperation for several components of the Norrin and Wnt7a/Wnt7b systems, and they reveal substantial regional heterogeneity in the extent to which partially redundant ligands, receptors, and coactivators maintain the BBB and BRB.

β-catenin signaling | vascular endothelial cells | mouse genetics | central nervous system

In many organs, vascular endothelial cells (ECs) develop specialized structures and functions that are tailored to the needs of the surrounding tissue (1, 2). This specialization is especially evident in the central nervous system (CNS), where ECs constitute a diffusion barrier—the blood–brain barrier (BBB) and the blood–retina barrier (BRB)—that protects neurons and glia from plasma contents. Although the principal cellular component of the BBB is the EC, BBB integrity also requires pericytes, astroglia, and neurons, which together with ECs comprise the neurovascular unit (3, 4). The distinctive features of CNS ECs that account for the BBB are: (*i*) the presence of tight junctions, which block intercellular passage of solutes; (*ii*) repression of transcytotic vesicle transport and an absence of fenestrations, which blocks transcellular movement of solutes; (*iii*) expression of transporters, such as the glucose transporter GLUT1, which permits the selective movement of small molecules from the serum to the CNS parenchyma; and (*iv*) expression of ATP-driven pumps, such as P-glycoprotein, to extrude toxic compounds from the CNS parenchyma.

How does each organ (or region within an organ) instruct resident ECs to adopt a molecular and cellular program appropriate to that tissue? In the CNS, canonical Wnt signaling (which we refer to hereafter as "β-catenin signaling") is required in ECs to develop and maintain the BBB and BRB. In postnatal CNS ECs, loss of β-catenin signaling leads to a loss of barrier competence, and restoration of β-catenin signaling leads to a restoration of the barrier state (5–7). In addition to its role in the BBB and BRB, β-catenin signaling also plays an essential role in CNS angiogenesis, with mutations in the same β-catenin signaling components leading to incomplete vascularization of the developing retina or brain (8–10).

β-Catenin signaling in the context of the CNS vasculature is mediated by Frizzled receptors on ECs that respond to Wnt7a and Wnt7b in the brain and spinal cord and to Norrin in the retina, brain, and spinal cord (5–11). In the mature cerebral cortex, *Wnt7a* and *Wnt7b* are expressed by astroglia, oligodendrocytes, and neurons; *Ndp* (the gene coding for Norrin) is expressed predominantly by astroglia, with lower expression in oligodendrocytes (12). In the retina, *Ndp* is expressed by Muller glia (11). The gene encoding Frizzled4 (Fz4), the principal receptor for Norrin signaling in the retina (8, 13), is expressed by ECs throughout the body. Additional Frizzled family members are inferred to play a partially redundant role with Fz4 in mediating Wnt7a and Wnt7b signaling in the brain and spinal cord (6, 7, 14).

Significance

The blood–brain barrier (BBB) and the blood–retina barrier (BRB) play essential roles in maintaining the health of the central nervous system. Two partially redundant ligand–receptor systems—the Norrin and Wnt7a/Wnt7b systems—activate β-catenin signaling in vascular endothelial cells to control BBB and BRB development and maintenance. The present study explores the partially overlapping roles of these two systems in the postnatal brain and retinal vasculatures. In the cerebellum, the two signaling systems are substantially redundant in maintaining the BBB, with isolated loss of some components, such as the ligand Wnt7a or the coactivator Tspan12, producing little or no barrier defect but combined loss of the two components producing a large defect in barrier integrity.

Author contributions: Y.W. and J.N. designed research; Y.W., C.C., and J.W. performed research; P.M.S., C.Z., and H.J.J. contributed new reagents/analytic tools; Y.W. and J.N. analyzed data; and J.N. wrote the paper.

Reviewers: C.G., Harvard University; and B.S.C., National Cancer Institute, National Institutes of Health.

The authors declare no conflict of interest.

[1]To whom correspondence should be addressed. Email: jnathans@jhmi.edu.

This article contains supporting information online at www.pnas.org/lookup/suppl/doi:10.1073/pnas.1813217115/-/DCSupplemental.

Published online November 26, 2018.

In CNS ECs, signaling via receptor (Frizzled) and coreceptor (Lrp5 or Lrp6) components is greatly enhanced by various integral membrane and glycosylphosphatidylinositol (GPI)-anchored coactivators (Fig. 1*A*). In the context of Norrin signaling, Tspan12, a member of the tetraspanin family of integral membrane proteins, is required for normal retinal angiogenesis (15, 16). Cell culture experiments also implicate Lgr4, a 7-transmembrane segment (7TM) protein, in Norrin signaling, although its role in vivo is not yet clear (17). In the context of Wnt7a and Wnt7b signaling, Gpr124, a 7TM protein, and Reck, a GPI-anchored protein, functionally interact with each other and with Wnt7a or Wnt7b, Frizzled, and Lrp5 or Lrp6 at the plasma membrane to enhance β-catenin signaling, a system that we refer to as "Wnt7a/Wnt7b signaling" (14, 18–20). Gpr124 and Reck are essential for CNS angiogenesis and BBB development in multiple brain and spinal cord regions (7, 14, 21–26). Gpr124 also functions to minimize BBB breakdown in mouse models of ischemic stroke and glioblastoma (27).

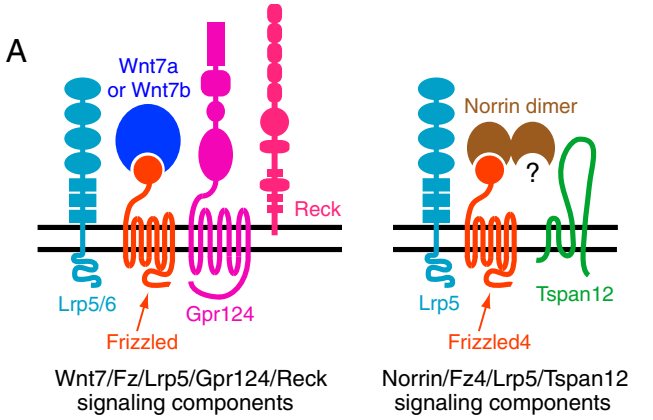

B Postnatal BBB/BRB development and maintenance (single gene loss-of-function phenotype)

	retina	brainstem	cerebellum	cerebral cortex
Ndp	S	U(R)	W(R)	U(R)
Tspan12	M	?	?	?
Wnt7a/Wnt7b	?	?	?	?
Gpr124	U	U(R)	U(R)	U(R)
Reck	U	U(R)	U(R)	U(R)
Fz4	S	U(R?)	M(R?)	U(R?)
Lrp5	M(R)	U(R)	U(R)	U(R)
Lrp6	U(R)	U(R)	U(R)	U(R)

S = strong
M = moderate
W = weak
U = undetectable
R = redundant

Fig. 1. Two distinct ligand–receptor systems for β-catenin signaling in CNS ECs. (*A*) Schematic illustration of the two β-catenin signaling systems active in CNS ECs: the Wnt7/Fz/Lrp5/Gpr124/Reck system (*Left*) and the Norrin/Fz4/Lrp5/Tspan12 system (*Right*). The disposition of ligand–receptor complexes at the plasma membrane (horizontal black lines) is shown with the extracellular space above and the intracellular space below. Whether both monomers within the Norrin dimer bind to a Fz4 receptor is not known at present; the schematic shows only one bound monomer. (*B*) Summary of the roles of different β-catenin signaling components in postnatal BBB and BRB development and maintenance. Effects on angiogenesis are excluded from this analysis. The results of loss-of-function mutations are indicated as strong, moderate, weak, undetectable, or redundant with one or more of the other listed genes. *Ndp* and *Tspan12* are specific to the Norrin/Fz4 ligand/receptor complex. *Wnt7a*, *Wnt7b*, *Gpr124*, and *Reck* are specific to the Wnt7/Fz ligand/receptor complex. *Fz4*, *Lrp5*, and *Lrp6* are shared by both complexes. Black letters indicate results of previous studies. Red question marks indicate the genes and functions analyzed in the present study. The redundancy associated with *Ndp*, *Gpr124*, and *Reck* derives from the severe phenotypes seen with the combined loss of *Ndp* and *Gpr124* and with the combined loss of *Ndp* and *Reck*. We note that the Reck mutant data comes from a hypomorphic allele rather than a full loss-of-function allele (14). In the brain, *Fz4* is assumed to be redundant with one or more other receptors because, relative to the BBB phenotype observed with loss of *Fz4* alone, there is a more severe BBB phenotype when loss of *Fz4* is combined with loss of *Ndp* (ligand) or *Lrp5* (coreceptor); these are marked as redundant with a question mark to indicate that the identities of the redundant Frizzleds are not yet known. Data are from refs. 7, 8, 14, 15, 18, and 28.

The existence of two classes of β-catenin ligands (Norrin and Wnt7a/Wnt7b) with distinct coactivator proteins dedicated to each (Tspan12 and Gpr124/Reck, respectively) suggests that different CNS regions may rely to different extents on one or the other to control angiogenesis and barrier formation and maintenance. Consistent with this idea, earlier studies found that angiogenesis in the retina is controlled largely or exclusively by the Norrin system (6, 8, 11, 15, 28) and that angiogenesis in the cerebral cortex and medial ganglionic eminences are controlled largely or exclusively by the Wnt7a/Wnt7b system (9, 10, 21–23). In contrast, angiogenesis in the hindbrain is impaired only when both systems are mutated (14, 18).

Redundancy between the Norrin and Wnt7a/Wnt7b systems is also observed in the postnatal brain. Whereas constitutive loss of Norrin produces only a mild reduction in barrier integrity in the postnatal cerebellum and olfactory bulb, and reduction in Wnt7a/Wnt7b signaling (due to conditional deletion of Gpr124 or partial inactivation of Reck) has no effect on postnatal CNS barrier integrity, the combined loss of Norrin and either Gpr124 or Reck leads to severe BBB defects in the cortex, thalamus, and brainstem (14, 18). Fig. 1*B* summarizes published data related to the effects of mutations in Norrin and Wnt7a/Wnt7b signaling components on postnatal BBB and BRB maintenance. To date, Tspan12 has been studied in the retina (15), but its function, if any, in the brain has not been explored.

At present, the role of the Wnt7a/Wnt7b system in BBB maintenance has largely been inferred from the phenotypes of Gpr124 and Reck loss-of-function mutations, either alone or in combination with mutations in Ndp or Fz4. However, Gpr124 has been reported to function in diverse processes, some of which may not reflect its role in β-catenin signaling. These include promoting EC survival via integrin signaling (29), mediating contact inhibition (30), enhancing EC responses to VEGF (31), and increasing cell adhesion (32). Similarly, the multidomain protein Reck includes a matrix metalloproteinase inhibitor domain that is distinct from the N-terminal domains implicated in Wnt7a/Wnt7b signaling and, therefore, some of Reck's loss-of-function phenotypes may reflect functions distinct from Wnt7a/Wnt7b signaling (33, 34). These considerations emphasize the importance of directly testing the effects of mutations in Wnt7a and/or Wnt7b alone and in combination with mutations in other genes coding for β-catenin signaling components.

The present studies were undertaken to more fully define the interactions between the Norrin and Wnt7a/Wnt7b signaling systems in CNS BBB maintenance and to explore the function of Tspan12 in BBB integrity, with the goal of filling the knowledge gaps indicated in Fig. 1*B*.

Results

Extensive Redundancy Between Norrin and Wnt7a in BBB Maintenance. The most direct approach for assessing interactions between the Norrin and Wnt7a/Wnt7b systems in BBB and BRB maintenance involves analyzing the phenotypes associated with loss-of-function mutations in the genes coding for their respective ligands. However, this analysis presents three technical challenges: (*i*) the likely redundancy between the highly homologous *Wnt7a* and *Wnt7b* genes, as suggested by their redundancy in the context of embryonic CNS angiogenesis (9); (*ii*) the sterility of $Wnt7a^{-/-}$ males and females; and (*iii*) the early lethality of $Wnt7b^{-/-}$ embryos, which

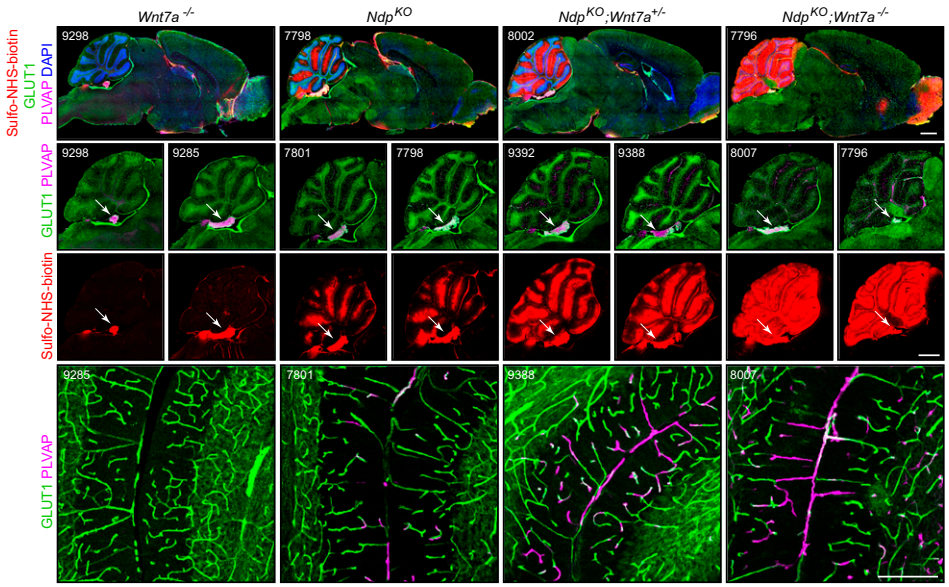

Fig. 2. Redundancy between Ndp and Wnt7a in the cerebellum and olfactory bulb. Coronal sections of ~P30 brains from representative examples of the indicated genotypes, immunostained for GLUT1 and PLVAP. Four-digit mouse identification numbers are in the upper corners of panels in this and other figures. The second and third rows show sections through the cerebellum from two representative brains for each genotype. The fourth row shows a representative region of the cerebellar vasculature at higher magnification. Arrows in the second and third rows indicate the choroid plexus. (Scale bars: 1 mm for rows 1–3; 200 μm for row 4.)

die before midgestation from a placental defect, thereby necessitating the use of a conditional *Wnt7b* allele for postnatal analyses.

To circumvent the third challenge, we began by investigating the effect of eliminating *Wnt7a*, either alone or in combination with *Ndp*. (*Ndp* is X-linked, and we will use "Ndp^{KO}" to refer both to males with hemizgous loss of *Ndp* and to females with homozygous loss of *Ndp*.) Fig. 2 shows sagittal brain sections—the standard format for the postnatal analyses described herein—from representative $Wnt7a^{-/-}$, Ndp^{KO}, Ndp^{KO};$Wnt7a^{+/-}$, and Ndp^{KO};$Wnt7a^{-/-}$ mice at P30, stained for: (*i*) GLUT1, an EC marker for the BBB state; (*ii*) plasmalemma vesicle-associated protein (PLVAP; a structural protein that comprises the diaphragm in EC fenestrae and transcytotic vesicles), an EC marker for the high permeability state; and (*iii*) covalent Sulfo-NHS-long-chain-biotin ("Sulfo-NHS-biotin") adducts. Sulfo-NHS-biotin is a marker for leakage of low molecular weight serum components into the CNS parenchyma; it was delivered to each mouse by intraperitoneal injection.

$Wnt7a^{-/-}$ brains are indistinguishable from WT controls with respect to the distribution of GLUT1, PLVAP, and Sulfo-NHS-biotin. (See *SI Appendix*, Fig. S1 for a representative WT brain.) In particular, conventional CNS ECs are uniformly $GLUT1^+/PLVAP^-$, and the only locations within the CNS where Sulfo-NHS-biotin accumulates outside of the vasculature is the choroid plexus (arrows in second and third rows of Fig. 2) and the circumventricular organs, small midline structures that are variably present in the sections shown here. Choroid plexus and circumventricular organ ECs are $GLUT1^-;PLVAP^+$ and are highly permeable.

As previously reported (7), Ndp^{KO} brains show a low level of BBB breakdown in the cerebellum, centered on the occasional ECs that have converted from $GLUT1^+/PLVAP^-$ to $GLUT1^-;PLVAP^+$ (Fig. 2, column 2). Ndp^{KO};$Wnt7a^{+/-}$and Ndp^{KO};$Wnt7a^{-/-}$ brains show progressively greater extents of BBB breakdown and EC marker conversion in the cerebellum. In Ndp^{KO};$Wnt7a^{-/-}$ brains, this phenotype is also observed in the olfactory bulb. Fig. 3, which quantifies the extent of $GLUT1^+/PLVAP^-$ to $GLUT1^-;PLVAP^+$ conversion of cerebellar ECs for all of the genotypes studied here, confirms the visual impression that, with loss of additional *Wnt7a* alleles in the Ndp^{KO} background, there is a step-wise increase in EC conversion from a barrier-competent state to a permeable state.

In sum, these data reveal a role for Wnt7a in BBB development and maintenance in the cerebellum and olfactory bulb, and

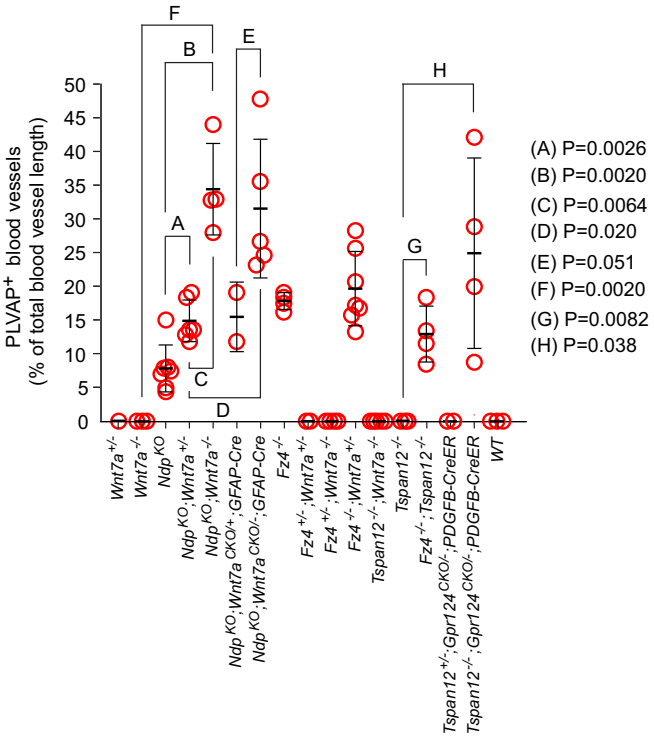

Fig. 3. Quantification of phenotypic conversion of cerebellar ECs from $GLUT1^+/PLVAP^-$ to $GLUT1^-/PLVAP^+$. For each of the indicated genotypes, the fraction of the cerebellar vasculature that was $GLUT1^-/PLVAP^+$ was determined as described in *Materials and Methods*. Each data point represents a different mouse. Bars indicate mean ± SD. *P* values for pairwise comparisons were calculated using the two-tailed Student's *t* test.

they demonstrate that Wnt7a and Norrin are largely redundant in this context.

Bergmann Glia Are the Principle Source of *Wnt7a* for Cerebellar BBB Maintenance. RNA sequencing (RNA-seq) on FACS-sorted cerebral cortical cells shows *Wnt7a* transcripts in a variety of cell types, and most abundantly in astroglia (12). Based on the expression of an alkaline phosphatase reporter knocked into the *Ndp* locus, the principal site of *Ndp* expression in the cerebral cortex is also astroglia, and in the cerebellum it is Bergmann glia (35). To functionally assess whether Bergmann glia are also the principal source of *Wnt7a* in the cerebellum, we generated mice lacking *Ndp* in all cells and lacking *Wnt7a* only in Bergmann glia. In these mice, recombination of a conditional *Wnt7a* allele by a *Gfap-Cre* driver [*Tg(GFAP-cre)25Mes*] (36) was judged to be specific to Bergmann glia because, in separate experiments, the combination of *Gfap-Cre* and a loxP-stop-loxP reporter at the *Rosa26* locus (*R26-LSL-mtdT-2A-H2B-GFP*) showed colocalization of reporter expression with S100-β, a marker for Bergmann glia, but not with NeuN or Calbindin, markers for granule cells and Purkinje cells, respectively (*SI Appendix*, Fig. S2). We note that multiple *Gfap-Cre* lines exist (see www.informatics.jax.org/recombinase/summary?driver=GFAP), and these lines exhibit a range of glial and neuronal expression patterns.

As seen in Fig. 4, Ndp^{KO};$Wnt7a^{CKO/+}$;*Gfap-Cre* mice exhibit a mild phenotype of cerebellar BBB breakdown and EC conversion from GLUT1$^+$/PLVAP$^-$ to GLUT1$^-$/PLVAP$^+$ that closely resembles the phenotype of Ndp^{KO};$Wnt7a^{+/-}$ mice (compare Fig. 2, column 3 to Fig. 4, column 1; see quantification in Fig. 3). Ndp^{KO}; $Wnt7a^{CKO/-}$;*Gfap-Cre* mice show a more severe phenotype of cerebellar BBB breakdown and EC conversion from GLUT1$^+$/PLVAP$^-$ to GLUT1$^-$/PLVAP$^+$ that closely resembles the phenotype of Ndp^{KO};$Wnt7a^{-/-}$ mice (compare Fig. 2, column 4 to Fig. 4, column 2; see quantification in Fig. 3). The near identity between the phenotypes resulting from constitutive or Bergmann glia-specific elimination of *Wnt7a* imply that most, and perhaps all, of the *Wnt7a* that drives BBB maintenance in the cerebellum is derived from Bergmann glia.

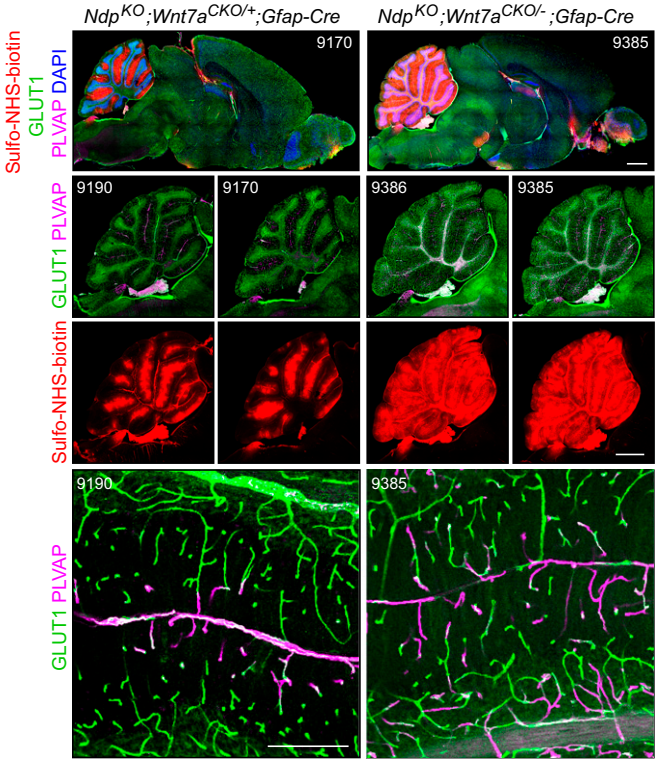

Fig. 4. In an Ndp^{KO} background, conditional knockout of *Wnt7a* with *Gfap-Cre* impairs cerebellar BBB maintenance. Coronal sections of ~P30 brains from representative examples of the indicated genotypes. The second and third rows show sections through the cerebellum from two representative brains for each genotype. The fourth row shows a representative region of the cerebellar vasculature at higher magnification. (Scale bars: 1 mm for rows 1–3; 200 μm for row 4.)

Loss of *Fz4* Sensitizes the CNS Vasculature to Loss of *Wnt7a*. To further assess the role of Wnt7a in BBB development and maintenance, we asked how the severity of the BBB phenotype changes with simultaneous reductions in *Wnt7a* and *Fz4*. Removing one copy each of *Fz4* and *Wnt7a* ($Fz4^{+/-}$;$Wnt7a^{+/-}$) did not alter BBB integrity (Fig. 5*A*, *Left* column). Removing one copy of *Fz4* and both copies of *Wnt7a* ($Fz4^{+/-}$;$Wnt7a^{-/-}$) produced a very low level of cerebellar EC conversion from GLUT1$^+$/PLVAP$^-$ to GLUT1$^-$/PLVAP$^+$ and a correspondingly low level of vascular leakage (Fig. 5*A*, second and third columns; quantified in Fig. 3). This phenotype was substantially milder than that associated with loss of *Fz4* alone (Fig. 5*A*, fourth column) or *Ndp* alone (Fig. 2, second column). Removing both copies of *Fz4* and one copy of *Wnt7a* ($Fz4^{-/-}$;$Wnt7a^{+/-}$) produced a phenotype similar to that observed in $Fz4^{-/-}$ mice, with vascular leakage largely confined to the cerebellum, olfactory bulb, and interpeduncular nuclei (Fig. 5*A*, *Right* column; quantified in Fig. 3).

Eliminating both *Fz4* and *Wnt7a* resulted in perinatal lethality, with no viable $Fz4^{-/-}$;$Wnt7a^{-/-}$ progeny among 175 that were genotyped from a $Fz4^{+/-}$;$Wnt7a^{+/-}$ intercross in which one-sixteenth should have been $Fz4^{-/-}$;$Wnt7a^{-/-}$ ($P = 0.0022$; two-tailed χ^2 test). Among embryonic day (E)17 embryos from the $Fz4^{+/-}$;$Wnt7a^{+/-}$ intercross, $Fz4^{-/-}$;$Wnt7a^{-/-}$ embryos were distinctive in exhibiting intracranial bleeding, a phenotype that had been seen previously in association with severe defects in CNS angiogenesis (e.g., ref. 21). $Fz4^{-/-}$;$Wnt7a^{-/-}$ brains showed bleeding in multiple locations, and these locations were associated with mild-to-moderate defects in vascularization, as seen in *SI Appendix*, Fig. S3 for the tectum. Overall, CNS vascularization was sparser in $Fz4^{-/-}$;$Wnt7a^{-/-}$ brains (Fig. 5*B*). In E17 $Fz4^{-/-}$;$Wnt7a^{-/-}$ brains, PLVAP is present in many ECs in the olfactory bulb and striatum, and lower but still detectable levels of PLVAP are present in ECs in the cerebral cortex. Additionally, in E17 $Fz4^{-/-}$;$Wnt7a^{-/-}$ brains, CLDN5 and GLUT1 were only partially anticorrelated with PLVAP, with many ECs expressing both PLVAP and GLUT1 and a smaller number expressing PLVAP and CLDN5 (Fig. 5*B*). This pattern contrasts with the adult pattern, in which CNS ECs with reduced levels of β-catenin signaling are generally either CLDN5$^+$/GLUT1$^+$/PLVAP$^-$ or CLDN5$^-$/GLUT1$^-$/PLVAP$^+$, and few or no ECs show an intermediate phenotype (e.g., Figs. 2 and 4). In E17 WT, $Fz4^{+/-}$;$Wnt7a^{-/-}$, and $Fz4^{-/-}$;$Wnt7a^{+/-}$ CNS ECs, PLVAP was undetectable or barely detectable and CLDN5 and GLUT1 were uniformly expressed.

The mild CNS vascularization defects in $Fz4^{-/-}$;$Wnt7a^{-/-}$ embryos are in contrast with the severe defects in *Gpr124* and *Reck* mutants and in EC-specific *Ctnnb1* (the gene coding for β-catenin) mutants (7), suggesting that additional Frizzled receptors and additional ligands—presumably Norrin and Wnt7b—were partially compensating for loss of *Fz4* and *Wnt7a*. Similarly, the incomplete conversion of ECs from CLDN5$^+$/GLUT1$^+$/PLVAP$^-$ to CLDN5$^-$/GLUT1$^-$/PLVAP$^+$ may reflect residual β-catenin signaling.

In sum, these data imply that: (*i*) Wnt7a and Fz4 function broadly in the prenatal CNS; (*ii*) this function is partially covered by redundant ligands and receptors; (*iii*) altered expression of CLDN5, GLUT1, and PLVAP—especially in the olfactory bulb and striatum—is a sensitive indicator of reduced β-catenin signaling

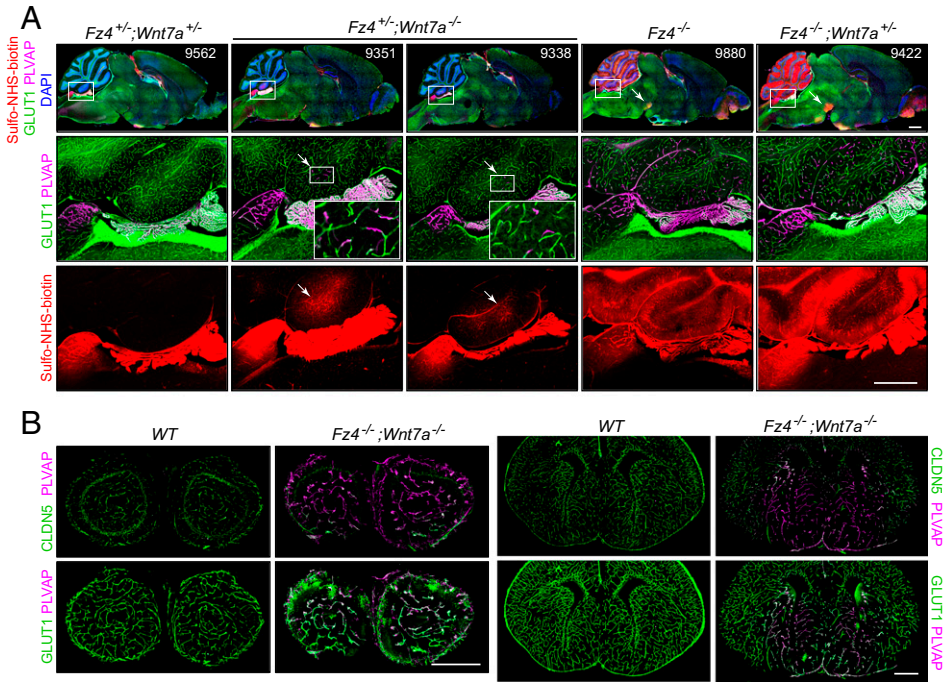

Fig. 5. Loss of *Fz4* synergizes with loss of Wnt7a in BBB maintenance. (*A*) Coronal sections of ∼P30 brains from representative examples of the indicated genotypes, immunostained for GLUT1 and PLVAP. Arrows in the *Right* two panels of the *Top* row point to Sulfo-NHS-biotin leakage in the interpeduncular nuclei. The second and third rows show an enlargement of the boxed region from each *Top* row image encompassing the ventral-most folia of the cerebellum and the adjacent choroid plexus. In the two $Fz4^{+/-}$;$Wnt7a^{-/-}$ panels, arrows in the second and third rows point to regions with mild Sulfo-NHS-biotin leakage and partial conversion of ECs, and boxed regions in the second row are enlarged as *Insets* and show capillary ECs that have converted from GLUT1$^+$/PLVAP$^-$ to GLUT1$^-$/PLVAP$^+$. (Scale bars: 1 mm in row 1; 500 μm in rows 2 and 3. *Insets* in row 2 are enlarged 3.7×.) (*B*) Coronal sections of E17 WT or $Fz4^{-/-}$;$Wnt7a^{-/-}$ brains, immunostained for CLDN5, GLUT1, and PLVAP. (Scale bars, 500 μm.)

during embryogenesis; and (*iv*) the all-or-none nature of the EC choice between CLDN5$^+$/GLUT1$^+$/PLVAP$^-$ to CLDN5$^-$/GLUT1$^-$/PLVAP$^+$ states is a feature of more mature CNS ECs.

Genetic Interactions Between Tspan12 and Other β-Catenin Signaling Components in the Brain. To assess the role of Tspan12 in BBB development and maintenance, we first examined $Tspan12^{-/-}$ mice. Postnatal day (P)12 and adult $Tspan12^{-/-}$ brains are indistinguishable from WT control brains in showing no Sulfo-NHS-biotin leakage into regions that are normally protected by the BBB and no detectable conversion of ECs from GLUT1$^+$/PLVAP$^-$ to GLUT1$^-$/PLVAP$^+$ (Fig. 6, column 1). The absence of a BBB phenotype in $Tspan12^{-/-}$ mice and the mild cerebellar leakage in Ndp^{KO} mice (Fig. 2, second column) parallels the relative severities of the retinal angiogenesis defects associated with these two genotypes, and is consistent with the current model in which Tspan12 augments Norrin signaling but is not absolutely required for it (15, 16).

Because Ndp^{KO};$Wnt7a^{-/-}$ mice exhibit a massive loss of BBB integrity in the cerebellum and olfactory bulb, we asked whether $Tspan12^{-/-}$;$Wnt7a^{-/-}$ mice exhibit BBB defects. Fig. 3 and *SI Appendix*, Fig. S4 show that $Tspan12^{-/-}$;$Wnt7a^{-/-}$ mice have a normal BBB, implying that loss of Tspan12 produces only a partial reduction in Norrin-dependent signaling so that the β-catenin signal remains above the critical threshold for BBB maintenance in this double mutant combination.

We next asked whether a more substantial reduction in Wnt7a/Wnt7b signaling in a $Tspan12^{-/-}$ background—produced by eliminating *Gpr124* in postnatal ECs (with *Pdgfb-CreER* and a $Gpr124^{CKO}$ allele)—could reduce the β-catenin signal below the critical threshold for BBB disruption (Fig. 6). While there was minimal conversion of cerebellar ECs from GLUT1$^+$/PLVAP$^-$ to GLUT1$^-$/PLVAP$^+$ in $Tspan12^{+/-}$;$Gpr124^{CKO/-}$;*Pdgfb-CreER* mice (Fig. 3), there was widespread low-level Sulfo-NHS-biotin labeling in the $Tspan12^{+/-}$;$Gpr124^{CKO/-}$;*Pdgfb-CreER* brain (Fig. 6, column 2). Eliminating *Gpr124* in postnatal ECs in a $Tspan12^{-/-}$ background ($Tspan12^{-/-}$;$Gpr124^{CKO/-}$;*Pdgfb-CreER*) produced severe Sulfo-NHS-biotin leakage in the hippocampus, superior colliculus, striatum, and brainstem, and milder leakage in the cerebral cortex, cerebellum, and hypothalamus, together with widespread conversion of ECs from GLUT1$^+$/PLVAP$^-$ to GLUT1$^-$/PLVAP$^+$ (Fig. 6, columns 3 and 4). This phenotype resembles the phenotype seen in postnatal Ndp^{KO};$Gpr124^{CKO/-}$;*Pdgfb-CreER* mice (18), and implies a role for Tspan12 in Norrin signaling in postnatal brain ECs.

Finally, we asked whether loss of both *Tspan12* and *Fz4* enhances the BBB phenotype compared with the loss of *Fz4* alone. Fig. 3 and *SI Appendix*, Fig. S5 show that the two genotypes exhibit indistinguishable distributions and severities of BBB loss, consistent with a model in which *Tspan12* acts exclusively to enhance Norrin-Fz4 signaling.

The Wnt7a/Wnt7b System Plays a Minimal Role in Retinal Vascular Development. As judged by publicly available RNA-seq datasets and published RT-PCR and in situ hybridization analyses in mice, the developing retina expresses *Wnt7a* at a low level and *Wnt7b* at a higher level; the adult retina expresses both *Wnt7a* and *Wnt7b* at a low level; and the developing lens expresses *Wnt7a* (37–39). To assess the possibility that the Wnt7a/Wnt7b system plays a role in retinal vascularization and BRB development and maintenance, we began by looking for a genetic interaction between *Wnt7a* and *Ndp* by comparing retina flat mounts from $Wnt7a^{-/-}$, Ndp^{KO}, and Ndp^{KO};$Wnt7a^{-/-}$ mice at P30 (Fig. 7*A*). In $Wnt7a^{-/-}$ retinas, ECs were uniformly GLUT1$^+$/PLVAP$^-$ and the vascular architecture was indistinguishable from that of WT retinas. In Ndp^{KO} retinas, ECs form numerous small clusters in place of intraretinal capillaries,

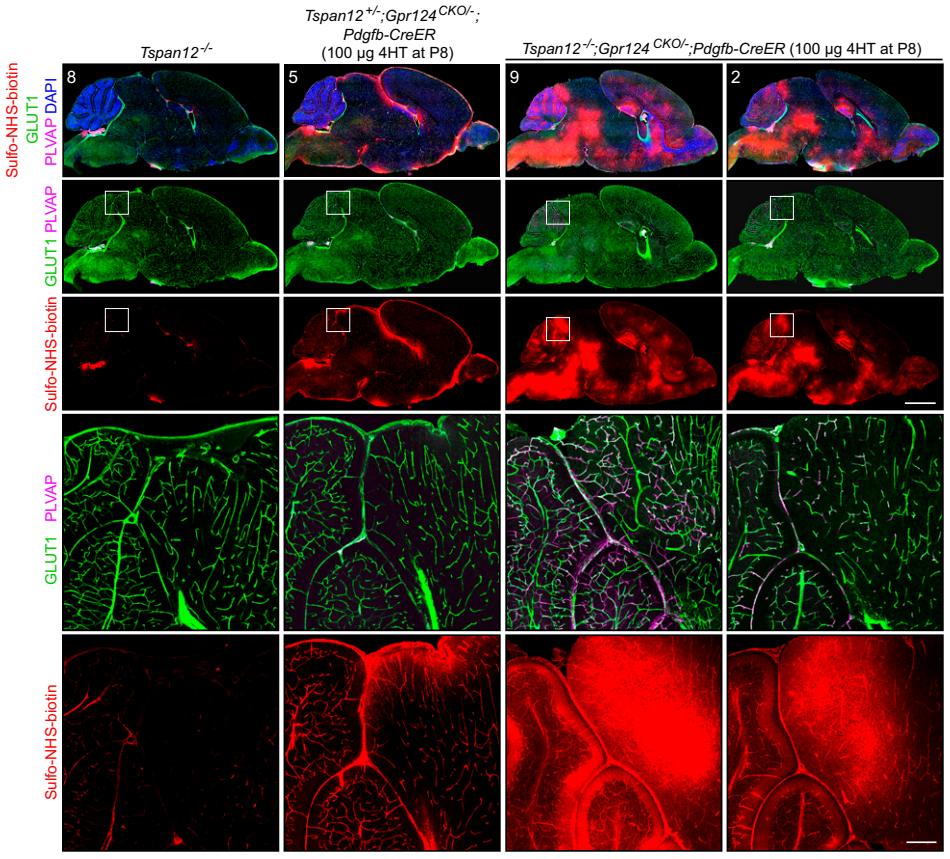

Fig. 6. Anatomic distribution of BBB breakdown with combined loss of *Tspan12* and *Gpr124* in CNS ECs. Coronal sections of P12 brains from representative examples of the indicated genotypes. Boxed regions in the second and third rows are enlarged in the fourth and fifth rows, and show GLUT1^{+}/PLVAP^{-} to GLUT1^{-}/PLVAP^{+} conversion and Sulfo-NHS-biotin leakage in the anterior cerebellum (left part of each image) and the superior colliculus (right part of each image). The two *Tspan12*$^{-/-}$;*Gpr124*$^{CKO/-}$;*Pdgfb-CreER* brains show the stereotyped regional distribution (with some variability in severity) of the BBB breakdown phenotype. 4HT was administered at P8 and brains were analyzed at P12. These experiments used a short time interval between 4HT injection and sacrifice because mice with combined postnatal loss of the Norrin and Wnt7a/Wnt7b systems do not survive more than several days to several weeks, depending on the 4HT dose and the extent of BBB loss. (Scale bars: 1 mm for rows 1–3; 200 μm for rows 4 and 5.)

and ECs in capillaries and veins are uniformly converted from GLUT1^{+}/PLVAP^{-} to GLUT1^{-}/PLVAP^{+}, while ECs in arteries and arterioles remain GLUT1^{+}/PLVAP^{-}. The *Ndp*^{KO} phenotype was unaltered by the additional loss of *Wnt7a*. While these data imply that Wnt7a plays a far smaller role in retinal vascular development and BRB maintenance than Norrin, the severity of the *Ndp*^{KO} phenotype leaves little room for a worsening of the phenotype with the further loss of *Wnt7a*.

The experiments presented in Figs. 2–6, together with those reported in ref. 7, imply that small decrements in β-catenin signaling—as seen, for example, in *Wnt7a*$^{-/-}$ or *Tspan12*$^{-/-}$ brains—have little or no effect if the β-catenin signal is not reduced below a critical threshold. To reduce β-catenin signaling via the Norrin system in a manner that might permit the observation of phenotypic effects caused by small additional decrements, we studied genetic interactions in a background of homozygous and heterozygous loss of *Tspan12*.

Tspan12$^{-/-}$ retinas resemble *Fz4*$^{-/-}$ and *Ndp*^{KO} retinas in exhibiting a complete conversion of venous and capillary ECs from GLUT1^{+}/PLVAP^{-} to GLUT1^{-}/PLVAP^{+} (Fig. 7*B*, *Right*). However, as reported previously (15), *Tspan12*$^{-/-}$ retinas exhibit an angiogenesis defect that is milder than that of *Fz4*$^{-/-}$ and *Ndp*^{KO} retinas, with partial vascularization of the inner retina and fewer EC clusters near the vitreal surface [in Fig. 7*B*, compare *Fz4*$^{-/-}$;*Tspan12*$^{+/-}$ (an example of a severe phenotype) with *Tspan12*$^{-/-}$]. Fig. 7*B* shows that *Tspan12*$^{-/-}$;*Wnt7a*$^{-/-}$ retinas exhibit a vascular phenotype that is indistinguishable from the *Tspan12*$^{-/-}$ phenotype, suggesting that *Wnt7a* produced by the retina and lens has little or no effect on retinal vascular anatomy. However, a limitation of this experiment is that the full conversion of *Tspan12*$^{-/-}$ vein and capillary ECs to a GLUT1^{-}/PLVAP^{+} state precludes an assessment of Wnt7a effects on the BRB phenotype.

In a second approach, we started with a *Tspan12*$^{+/-}$ genetic background, which only minimally reduces β-catenin signaling and leaves retinal ECs in a GLUT1^{+}/PLVAP^{-} state, and then studied the effect of impairing the Wnt7a/Wnt7b system. *Tspan12*$^{+/-}$ mice and *Tspan12*$^{+/-}$;*Wnt7a*$^{-/-}$ mice showed no abnormalities in retinal vascularization and no conversion of retinal capillary and venous ECs from GLUT1^{+}/PLVAP^{-} to GLUT1^{-}/PLVAP^{+} (Fig. 7*C*). *Gpr124*$^{CKO/-}$;*Pdgfb-CreER* mice also show no retinal vascular phenotype at P10 (Fig. 7*C*) or at P30. However, *Tspan12*$^{+/-}$;*Gpr124*$^{CKO/-}$;*Pdgfb-CreER* mice show a partial conversion of capillary and venous ECs from GLUT1^{+}/PLVAP^{-} to GLUT1^{-}/PLVAP^{+} (Fig. 7*C*, *Lower* row). [The BBB disruption that results from the combined postnatal loss of *Tspan12* and *Gpr124* (as seen in Fig. 6), limits the time window available between 4HT injection (P6) and phenotypic analysis (P10) for the experimental series shown in Fig. 7*C*, and this may lead to an underestimation of the full extent of the retinal phenotype.] Fig. 7*C* also shows that, at P10, *Tspan12*$^{-/-}$ retinas have already acquired the GLUT1^{-}/PLVAP^{+} phenotype that they exhibit at P30 (Fig. 7*B*), and that this phenotype and the modestly reduced vascular density characteristic of the P10 *Tspan12*$^{-/-}$ retinal vasculature are unaffected by the additional loss of *Gpr124*.

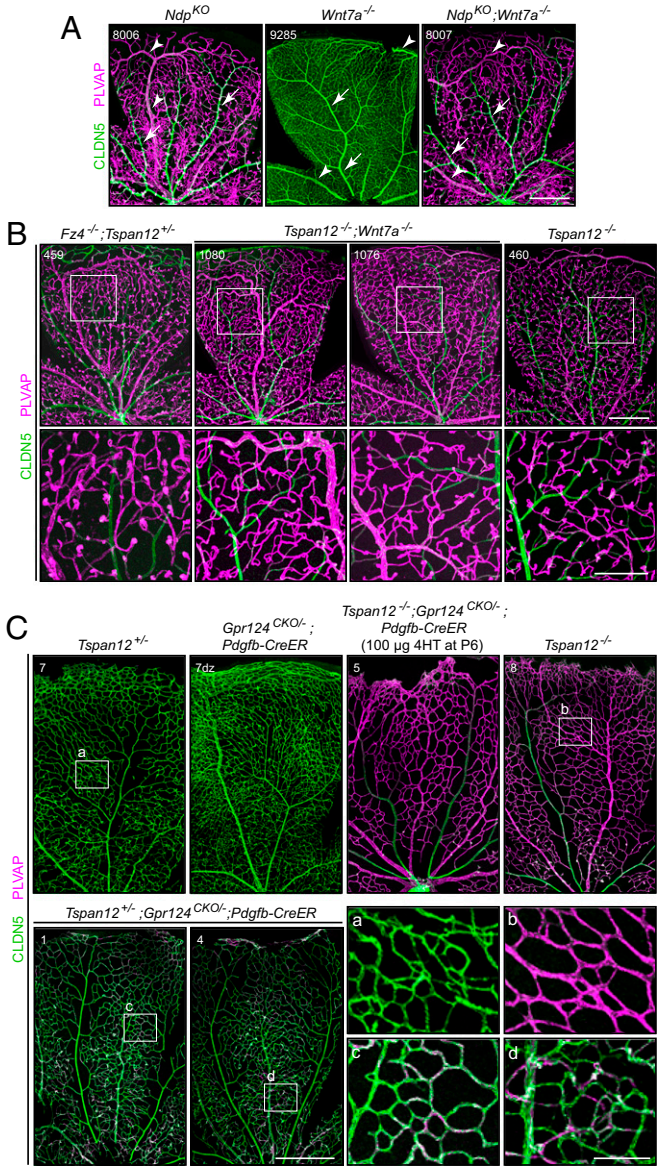

Fig. 7. The Wnt7a/Wnt7b system has only minimal effects on retinal vascular development and BRB maintenance. Flatmounts of P30 (*A* and *B*) and P10 (*C*) retinas from representative examples of the indicated genotypes. (*A*) The Ndp^{KO} and Ndp^{KO};$Wnt7a^{-/-}$ vasculature lacks intraretinal capillaries and exhibits numerous EC clusters just beneath the vitreal face of the retina. The $Wnt7a^{-/-}$ vasculature is indistinguishable from WT. In Ndp^{KO} and Ndp^{KO};$Wnt7a^{-/-}$ retinas, ECs in capillaries and veins (arrowheads) are converted from $GLUT1^{+}$/$PLVAP^{-}$ to $GLUT1^{-}$/$PLVAP^{+}$, whereas arteries (arrows) and arterioles remain $GLUT1^{+}$/$PLVAP^{-}$. (Scale bar, 500 µm.) (*B*) The $Fz4^{-/-}$;$Tspan12^{+/-}$ retina is an example of a severe phenotype, with no intraretinal capillaries and many EC clusters just beneath the vitreal face of the retina. In the $Tspan12^{-/-}$ retina (far *Right*), ECs in capillaries and veins are converted from $GLUT1^{+}$/$PLVAP^{-}$ to $GLUT1^{-}$/$PLVAP^{+}$, but vascular growth into the retina and intraretinal capillary formation are only partially impaired, with few EC clusters. $Tspan12^{-/-}$;$Wnt7a^{-/-}$ retinas exhibit a retinal vascular phenotype indistinguishable from $Tspan12^{-/-}$ retinas; two examples are shown. Boxed regions in the *Upper* images are enlarged in the *Lower* images. [Scale bars, 500 µm (*Upper*), 200 µm (*Lower*).] (*C*) Postnatal loss of *Gpr124* ($Gpr124^{CKO/-}$; *Pdgfb-CreER* with 4HT at P6) synergizes with heterozygosity for *Tspan12* to produce a partial conversion from $GLUT1^{+}$/$PLVAP^{-}$ to $GLUT1^{-}$/$PLVAP^{+}$ in the developing (P10) retinal vasculature. Boxed regions labeled *a*–*d* are enlarged in the *Lower Right* images. (Scale bars, 500 µm for low magnification, 100 µm for enlarged images.)

Taken together, these experiments imply that Wnt7a/Wnt7b signaling is active at a low level in the retinal vasculature, and that its loss can only be observed if the Norrin system is partially compromised. It is presently unknown whether the lower level of Wnt7a/Wnt7b signaling in the retina reflects a lower level of Wnt7 ligands compared with Norrin, a lower level of Gpr124 or Reck compared with Tspan12, the presence of extracellular Wnt inhibitors, or some other factors.

Specificity of Tspan12 Action in a Cell Culture System. To date, *Tspan12* loss-of-function phenotypes have been interpreted on the assumption that Tspan12 acts only to augment Norrin signaling via its receptor Fz4. This model is based on the observation that Tspan12 has no effect on Wnt3a, Wnt5a, or Wnt7b signaling in the same cell culture system in which it augments Norrin signaling by ∼five- to sevenfold (15, 16). In the present context, it is of interest to systematically determine whether Tspan12 can augment signaling via any of the other Wnts.

We addressed this question by measuring the level of β-catenin signaling in a stable luciferase reporter cell line [Super Top Flash (STF) cells] with or without an N-terminal Rim-epitope tagged Fz4 and Tspan12 and with no coexpressed ligand or with coexpression of each of the 19 mammalian Wnts or Norrin (Fig. 8). We used Rim-tagged Fz4 rather than untagged Fz4, because—compared with untagged Fz4—Rim-tagged Fz4 exhibits greater responsiveness to Tspan12 (∼30-fold) despite an overall decrease of ∼8-fold in signal amplitude (Fig. 8, *Inset*). Immunoblotting shows that the majority of the Rim-tagged Fz4 proteins have a lower mobility in SDS/PAGE, suggesting that only a minority of the Rim-tagged Fz4 proteins follow the correct pathway of biosynthesis and intracellular trafficking (*SI Appendix*, Fig. S6). RNA sequencing has shown that STF cells express many Frizzleds at low level, and this likely accounts for the nonzero luciferase signal observed in the absence of Frizzled transfection (7). As seen in Fig. 8, the magnitude of luciferase activation depended on which Wnt was expressed. For each of the 19 Wnts there was either no change or a modest inhibition in β-catenin signaling in the presence of Tspan12.

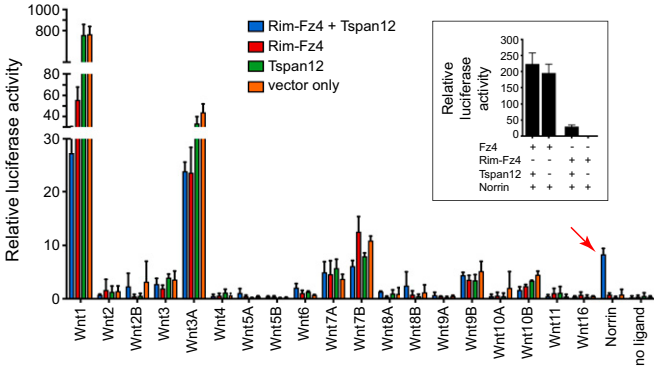

Fig. 8. Specificity of Tspan12 for Norrin vs. Wnts in a cell-based assay of β-catenin signaling. STF cells were transiently transfected with plasmids coding for Norrin, the indicated Wnt, or an empty vector together with the indicated combination of plasmids coding for Rim-Fz4, and/or Tspan12, or empty vector, together with *Renilla* luciferase. The ratio of firefly luciferase activity from the stably integrated STF reporter relative to *Renilla* luciferase activity is shown. Norrin is the only ligand that shows an enhanced luciferase signal in response to *Tspan12* expression (red arrow). (*Inset*) Comparison between untagged Frizzled4 and Rim-Fz4, with or without cotransfected Tspan12. Mean values ± SD are shown. Statistical significance values for pairwise comparisons with the vector-only controls are shown in *SI Appendix*, Table S1. The inhibition of some Wnts (e.g., Wnt1 and Wnt3a) by some Frizzleds may represent competition for essential signaling components by overexpressed proteins.

NEUROSCIENCE

The only ligand that showed an enhanced signal in the presence of Tspan12 was Norrin (Fig. 8, arrow).

Taken together, these data support the original model that Tspan12 specifically enhances Norrin signaling (15), and they mirror the results of analogous STF experiments showing that Gpr124 and Reck specifically enhance Wnt7a and Wnt7b signaling (14, 18–20, 25).

Discussion

The experiments reported here fill several knowledge gaps regarding β-catenin signaling and BBB/BRB development and maintenance (Fig. 9).

First, we find that the role of Tspan12 in BBB maintenance resembles the role of Norrin, with two informative differences. One difference is that loss of *Ndp* produces a readily detectable defect in the cerebellar BBB, whereas loss of *Tspan12* is associated with a normal cerebellar BBB. This pattern parallels the more severe retinal angiogenesis defect produced by loss of *Ndp* compared with loss of *Tspan12* (15). These observations imply that in both cerebellar and retinal ECs loss of *Ndp* produces a larger decrement in β-catenin signaling than loss of *Tspan12*. A similar difference is seen in the relative severities of cerebellar BBB phenotypes produced by double-mutant combinations with *Fz4*. For *Ndp*, the relative severities of the BBB phenotypes are Ndp^{KO} (mild) < $Fz4^{-/-}$ (moderate) < Ndp^{KO};$Fz4^{-/-}$ (severe) (see figure 4 of ref. 7), whereas for *Tspan12* the relative severities are $Tspan12^{-/-}$ (no defect) << $Fz4^{-/-}$ (moderate) ~ $Tspan12^{-/-}$;$Fz4^{-/-}$ (moderate). Taken together, these data are consistent with a model in which: (*i*) Norrin signals mostly through Fz4, with potentially minor contribution from at least one other receptor, possibly Lgr4 (17); (*ii*) Tspan12 acts only in association with Fz4 and Norrin; and (*iii*) Tspan12 augments, but is not absolutely required for, Norrin signaling and, therefore, loss of Tspan12 reduces but does not eliminate Norrin signaling. Points (*i*) and (*iii*) are consistent with cell culture signaling experiments in refs. 15 and 16.

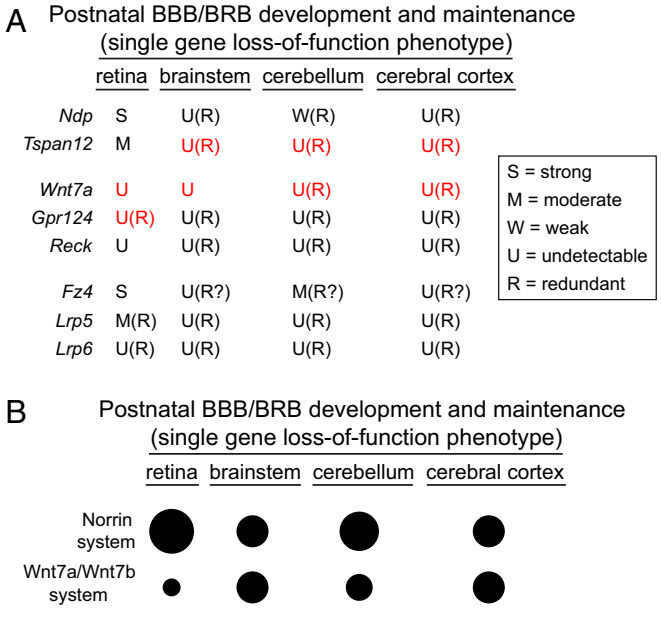

Fig. 9. Summary of the activities of the Norrin system vs. the Wnt7a/Wnt7b system in postnatal BBB and BRB development and maintenance. (*A*) Summary of the actions of each component, as organized in Fig. 1*B*. Effects on angiogenesis are excluded from this analysis. Red lettering indicates conclusions derived from data presented here. (*B*) Relative importance of the Norrin and the Wnt7a/Wnt7b systems in the retina, brainstem, cerebellum, and cerebral cortex, based on the data presented here and in the references cited in the legend to Fig. 1*B*.

Second, we find that Wnt7a promotes BBB maintenance in a manner that is partially redundant with the Norrin signaling system, as predicted from earlier work on Gpr124 and Reck. Earlier experiments showed that eliminating *Gpr124* or *Reck* together with *Ndp* leads to BBB disruption in the cerebellum, cortex, and brainstem (14, 18). We show here that eliminating *Wnt7a* together with *Ndp* also leads to BBB disruption in the cerebellum, while sparing the cortex and brainstem. The milder phenotype seen with loss of *Wnt7a* likely reflects the action of *Wnt7b*. Additionally, these experiments imply that the Wnt7a/Wnt7b system plays only a minor role in development and barrier integrity in the retina, most likely via the action of *Wnt7b*, which is expressed at higher levels in the developing retina that is *Wnt7a*.

Third, the *Gfap-Cre* experiments imply that, for maintenance of the cerebellar BBB, Bergmann glia serve as the principal source of Wnt7a. Earlier studies of *Ndp* expression using a *Ndp* reporter knockin allele showed that Bergmann glia, Muller glia, and astroglia are the principal sites of *Ndp* expression in the postnatal cerebellum, retina, and cortical and subcortical structures, respectively (35). Taken together, these observations imply that the Wnt7a- and Norrin-dependent β-catenin signal that controls BBB/BRB maintenance in the cerebellum and retina involves communication from glia to ECs.

Regional Anatomy and Threshold Effects in β-Catenin Signaling Systems for BBB/BRB Maintenance. Regional differences in the redundancy of the Norrin and Wnt7a/Wnt7b signaling systems divide the CNS into territories with different responses to loss-of-function mutations in β-catenin ligands, receptors, and coactivators (Fig. 9). In the retina, the Norrin system plays a predominant role, with a low level of signaling from the Wnt7a/Wnt7b system. This bias influences the spectrum of retinal vascular diseases caused by mutations in genes coding for β-catenin signaling components. Hemizygous loss-of-function mutations in *NDP* cause Norrie disease, heterozygous loss-of-function mutations in *CTNNB1*, *FZD4*, *TSPAN12*, or *LRP5* cause familial exudative vitreoretinopathy (FEVR), and compound heterozygous or homozygous mutations in *LRP5* cause FEVR or osteoporosis/pseudoglioma syndrome (40–49). There are also individuals with retinal vascular disease who have mutations in both copies of *FZD4* or *TSPAN12*, or in two different genes in the Norrin signaling system (48, 50–53). For retinal vascular diseases caused by mutations in genes coding for signaling components that are unique to the Norrin system (*NDP* and *TSPAN12*), the low level of redundant signaling from the Wnt7a/Wnt7b system is probably essential for revealing the disease phenotype.

In the mouse brain, region-specific variation in redundancy between the Norrin and Wnt7a/Wnt7b systems places the cerebellum and olfactory bulb at greatest risk for decrements in Norrin signaling. If these or other regions in the human brain are similarly dependent on Norrin signaling for BBB maintenance, that could explain the elevated incidence of epilepsy and other neurologic symptoms among Norrie disease patients (54). This line of reasoning also suggests that the enhanced BBB breakdown resulting from loss of *Gpr124* in models of stroke and glioblastoma (27) might show regional variations based on regional variations in the strength of β-catenin signaling and the redundancy of the Norrin and Wnt7a/Wnt7b systems. Because BBB breakdown frequently accompanies a variety of neurologic disorders—including head trauma, stroke, multiple sclerosis, Alzheimer's disease, epilepsy, and infection (4, 55)—it would be of interest to examine postmortem or surgical brain tissue for evidence of altered β-catenin signaling in human CNS ECs.

The work reported here, together with previous studies that explored the interactions between the Norrin and Wnt7a/Wnt7b signaling systems, raise a number of intriguing questions. Are there homeostatic interactions within or between the two signaling

systems that partially compensate for reduced or excessive levels of β-catenin signaling, resulting from perturbations of one or both systems? How are Norrin and Wnt7a/Wnt7b receptor complexes organized on the surface of ECs that are receiving or are able to receive both signals? Are the signals that are delivered to the cell interior by activation of Norrin/Fz4/Tspan12/Lrp5(Lrp6) and Wnt7a(Wnt7b)/Fz/Gpr124/Reck/Lrp5(Lrp6) signaling complexes identical, or are there effects of one or both signals in addition to β-catenin stabilization?

Continuous Versus Discrete Responses to β-Catenin Signaling. In the adult CNS vasculature, a suprathreshold level of β-catenin signaling maintains the BBB state, and reductions in β-catenin signaling below that threshold lead to increases in vascular permeability. When viewed macroscopically, BBB function appears to vary continuously with the strength of the β-catenin signal. However, when viewed microscopically, the BBB phenotype in the postnatal vasculature appears to be quantized: progressive reductions in β-catenin signaling lead to the conversion of a larger fraction of ECs from a GLUT1^{+}/PLVAP^{-} state to a GLUT1^{-}/PLVAP^{+} state. It is interesting that fetal ECs exhibit intermediate states of GLUT1 and PLVAP accumulation, suggesting that, as CNS ECs mature, they acquire positive feedback systems that favor the gene expression patterns underlying the GLUT1^{+}/PLVAP^{-} or GLUT1^{-}/PLVAP^{+} states while suppressing intermediate states of gene expression.

Materials and Methods

Mice. The following mouse alleles were used: *Fz4*$^{-}$ (8), *Ndp*$^{-}$ (11); *Pdgfb-CreER* (56), *Tspan12*$^{-}$ (57), *Wnt7a*$^{-}$ (9), *Gpr124*$^{-}$ and *Gpr124*^{CKO} (23), *R26-LSL-tdTomato-2A-H2B-GFP* (*SI Appendix*, Fig. S2), and *Gfap-Cre* [*Tg(Gfap-Cre)25Mes/J; JAX 004600*] (36). All mice were housed and handled according to the approved Institutional Animal Care and Use Committee protocol MO16M369 of the Johns Hopkins Medical Institutions.

To construct the *R26-LSL-tdTomato-2A-H2B-GFP Cre* reporter, the following elements were inserted (in the order listed) into a standard Rosa26 targeting vector: a CAG promoter, an LSL cassette that includes three tandem poly-adenylation signals, an ORF coding for a membrane tethered tdTomato with a 3×Myc epitope tag, a 2A peptide, and a histone H2B-GFP with a 3×HA epitope, a bovine growth hormone 3′UTR, and an *frt-phosphoglycerate kinase (PGK)-neomycin (Neo)-frt* (FNF) cassette. The targeting construct with a flanking Diphteria toxin-A coding sequence was electroporated into R1 ES cells, which were then subjected to G418 selection. Clones harboring the targeted allele were identified by Southern blot hybridization, karyotyped, and injected into blastocysts. Germline transmission to progeny of founder males was determined by PCR.

Antibodies and Other Reagents. The following reagents were used for tissue immunohistochemistry and immunoblotting: rabbit anti-GLUT1 (Thermo Fisher Scientific RB-9052-P1); rat anti-mouse PLVAP/MECA-32 (BD Biosciences 553849); mouse anti-CLDN5, Alexa Fluor 488 conjugate (Thermo Fisher Scientific 352588); Texas Red streptavidin (Vector Laboratories SA-5006); rabbit anti-GFP, Alexa Fluor 488 conjugate (Thermo Fisher Scientific A21311); chicken anti-GFP (Abcam ab13970); rabbit anti-6×Myc (JH6204); rabbit anti-calbindin (Swant CB-38); rabbit anti–S100-β (Abcam ab52642); rabbit anti-GFAP (NeoMarkers RB-087-A); mouse anti-NeuN (Chemicon MAB377); mouse mAb anti-Fz4 (Thermo-Fisher MA5-24377); mouse mAb anti-RIM (mAb 3F4) (58); mouse mAb antiactin (Millipore/Sigma MAB1501). Alexa Fluor-labeled secondary antibodies and GS Lectin (Isolectin GS-IB4) were from Thermo Fisher Scientific. Sulfo-NHS-biotin was from Thermo Fisher Scientific (catalog #21217).

Tissue Processing and Immunohistochemistry. Tissues were prepared and processed for immunohistochemical analysis as described in refs. 6 and 7. Mice were injected intraperitoneally with Sulfo-NHS-biotin (100 μL of 20 mg/mL Sulfo-NHS-biotin in PBS for P10–P12 mice, and 200 μL of 20 mg/mL Sulfo-NHS-biotin in PBS for P30 mice) at least 10 min before being killed. Mice were deeply anesthetized with ketamine and xylazine and then perfused via the cardiac route with 1% PFA in PBS without calcium or magnesium, and the brains were dissected and dehydrated in 100% MeOH overnight at 4 °C. Tissues were rehydrated the following day in 1× PBS at 4 °C for at least 3 h before embedding in 3% agarose. Tissue sections of 100- to 200-μm thickness were cut using a vibratome (Leica). For retina flatmounts, intact eyes were immersion fixed in 1% PFA in PBS at room temperature for 1 h, and then the retinas were dissected and processed as described below.

Sections were incubated overnight with primary antibodies or Texas Red streptavidin diluted in 1× PBSTC (1× PBS + 1% Triton X-100 + 0.1 mM $CaCl_2$) + 10% normal goat serum. Incubation and washing steps were performed at 4 °C. Sections were washed at least three times with 1× PBSTC over the course of 6 h, and subsequently incubated overnight with secondary antibodies diluted in 1× PBSTC + 10% normal goat serum. If a primary rat antibody was used, secondary antibodies were additionally incubated with 1% normal mouse serum as a blocking agent. The next day, sections were washed at least three times with 1× PBSTC over the course of 6 h, and flat-mounted using Fluoromount G (EM Sciences 17984–25). Sections were imaged using a Zeiss LSM700 confocal microscope, and processed with ImageJ, Adobe Photoshop, and Adobe Illustrator software.

4HT Preparation and Administration. Solid 4HT (Sigma-Aldrich H7904) was dissolved in an ethanol:sunflower seed oil (Sigma-Aldrich S5007) mixture (1:10 vol:vol) to a final concentration of 2 mg/mL and stored in aliquots at −80 °C. Thawed aliquots were diluted to a final concentration of 1 mg/mL 4HT. All injections were performed intraperitoneally.

Quantification of Cerebellar CLDN5 and PLVAP. For quantifying GLUT1 vs. PLVAP expression in cerebellar ECs, 150- to 180-μm-thick coronal vibratome sections were stained with anti-GLUT1, anti-PLVAP, and DAPI. Confocal images were scanned at 10-μm intervals along the *z* axis, of which four adjacent images were *z*-stacked. Starting with each *z*-stacked coronal image of the brain (as seen in Fig. 2), a rectangle 180 μm in width that spans the anterior to posterior extent of the cerebellum (~4 mm; parallel to the horizontal axis in Fig. 2) was centered on the middle of the vertical axis of the cerebellum (the vertical axis in Fig. 2). Using the pencil tool in Adobe Illustrator, all of the PLVAP^{+} vessels and all of the GLUT1^{+} vessels were separately traced in the area within that rectangle. The lengths of the PLVAP^{+}-traced vessels and the lengths of the GLUT1^{+} vessels were separately quantified by calculating pixel coverage as a fraction of the total area using ImageJ. The vascular density for PLVAP^{+} vessels was then divided by the sum of GLUT1^{+} and PLVAP^{+} vascular density for each rectangle.

The R software package was used to generate plots and to perform statistical analysis (59). The mean ± SDs are shown. Statistical significance was determined by the unpaired *t* test.

GLUT1 and PLVAP expression were quantified rather than Sulfo-NHS-biotin leakage because the former is a direct molecular readout of gene expression, whereas the signal from Sulfo-NHS-biotin leakage depends additionally on the efficiency of transfer of Sulfo-NHS-biotin from the peritoneal cavity to serum and on the uniformity of vascular perfusion. We also note that, when tissues are viewed at high magnification, the local spread of Sulfo-NHS-biotin within CNS tissue can lead to images in which Sulfo-NHS-biotin originates from permeable capillaries above or below the imaged *z*-planes.

Luciferase Assays. Dual luciferase assays were performed as described previously (8). Briefly, STF cells were plated on 96-well plates at a confluency of 30–40%. The following day, fresh DMEM/F-12 (Thermo Fisher Scientific 12500) supplemented with 10% FBS was replaced in each of the wells. Three hours later, cells were transfected in triplicate with expression plasmids (240 ng of DNA per three wells) using FuGENE HD Transfection Reagent (Promega E2311). The DNA master mix (unless otherwise specified) included: 1.5 ng of the internal control *Renilla* luciferase plasmid (pRL-TK), and 60 ng each of the pRK5 expression plasmids for Rim-Fz4, Norrin, Tspan12, and/or control vector. Forty-eight hours posttransfection, cells were harvested in 1× Passive Lysis Buffer (Promega E194A) for 20 min at room temperature. Lysates were used to measure firefly and *Renilla* luciferase activity using the Dual-Luciferase Reporter Assay System (Promega E1910) and a Turner BioSystems Luminometer (TD-20/20). Relative luciferase activity was calculated by normalizing firefly/*Renilla* values. GraphPad Prism 7 software was used to generate plots and perform statistical analysis. The mean ± SDs are shown.

ACKNOWLEDGMENTS. We thank Tom Spencer for the gift of *Wnt7a*$^{-}$ mice, and Amir Rattner for helpful discussions and assistance with statistical analyses. This work was supported by the Howard Hughes Medical Institute (J.N.), National Eye Institute Grants R01 EY018637 (to J.N.) and R01 EY024261 (to H.J.J.), and the Arnold and Mabel Beckman Foundation (J.N.).

1. Aird WC (2012) Endothelial cell heterogeneity. *Cold Spring Harb Perspect Med* 2: a006429.
2. Potente M, Mäkinen T (2017) Vascular heterogeneity and specialization in development and disease. *Nat Rev Mol Cell Biol* 18:477–494.
3. Daneman R, Prat A (2015) The blood-brain barrier. *Cold Spring Harb Perspect Biol* 7: a020412.
4. Zhao Z, Nelson AR, Betsholtz C, Zlokovic BV (2015) Establishment and dysfunction of the blood-brain barrier. *Cell* 163:1064–1078.
5. Liebner S, et al. (2008) Wnt/beta-catenin signaling controls development of the blood-brain barrier. *J Cell Biol* 183:409–417.
6. Wang Y, et al. (2012) Norrin/Frizzled4 signaling in retinal vascular development and blood brain barrier plasticity. *Cell* 151:1332–1344.
7. Zhou Y, et al. (2014) Canonical WNT signaling components in vascular development and barrier formation. *J Clin Invest* 124:3825–3846.
8. Xu Q, et al. (2004) Vascular development in the retina and inner ear: Control by norrin and frizzled-4, a high-affinity ligand-receptor pair. *Cell* 116:883–895.
9. Stenman JM, et al. (2008) Canonical Wnt signaling regulates organ-specific assembly and differentiation of CNS vasculature. *Science* 322:1247–1250.
10. Daneman R, et al. (2009) Wnt/beta-catenin signaling is required for CNS, but not non-CNS, angiogenesis. *Proc Natl Acad Sci USA* 106:641–646.
11. Ye X, et al. (2009) Norrin, frizzled-4, and Lrp5 signaling in endothelial cells controls a genetic program for retinal vascularization. *Cell* 139:285–298.
12. Zhang Y, et al. (2014) An RNA-sequencing transcriptome and splicing database of glia, neurons, and vascular cells of the cerebral cortex. *J Neurosci* 34:11929–11947.
13. Smallwood PM, Williams J, Xu Q, Leahy DJ, Nathans J (2007) Mutational analysis of norrin-frizzled4 recognition. *J Biol Chem* 282:4057–4068.
14. Cho C, Smallwood PM, Nathans J (2017) Reck and Gpr124 are essential receptor cofactors for Wnt7a/Wnt7b-specific signaling in mammalian CNS angiogenesis and blood-brain barrier regulation. *Neuron* 95:1056–1073.e5.
15. Junge HJ, et al. (2009) TSPAN12 regulates retinal vascular development by promoting Norrin- but not Wnt-induced FZD4/beta-catenin signaling. *Cell* 139:299–311.
16. Lai MB, et al. (2017) TSPAN12 is a Norrin co-receptor that amplifies frizzled4 ligand selectivity and signaling. *Cell Rep* 19:2809–2822.
17. Deng C, et al. (2013) Multi-functional norrin is a ligand for the LGR4 receptor. *J Cell Sci* 126:2060–2068.
18. Zhou Y, Nathans J (2014) Gpr124 controls CNS angiogenesis and blood-brain barrier integrity by promoting ligand-specific canonical wnt signaling. *Dev Cell* 31:248–256.
19. Posokhova E, et al. (2015) GPR124 functions as a WNT7-specific coactivator of canonical β-catenin signaling. *Cell Rep* 10:123–130.
20. Eubelen M, et al. (2018) A molecular mechanism for Wnt ligand-specific signaling. *Science* 361:eaat1178.
21. Kuhnert F, et al. (2010) Essential regulation of CNS angiogenesis by the orphan G protein-coupled receptor GPR124. *Science* 330:985–989.
22. Anderson KD, et al. (2011) Angiogenic sprouting into neural tissue requires Gpr124, an orphan G protein-coupled receptor. *Proc Natl Acad Sci USA* 108:2807–2812.
23. Cullen M, et al. (2011) GPR124, an orphan G protein-coupled receptor, is required for CNS-specific vascularization and establishment of the blood-brain barrier. *Proc Natl Acad Sci USA* 108:5759–5764.
24. de Almeida GM, et al. (2015) Critical roles for murine Reck in the regulation of vascular patterning and stabilization. *Sci Rep* 5:17860.
25. Vanhollebeke B, et al. (2015) Tip cell-specific requirement for an atypical Gpr124- and Reck-dependent Wnt/β-catenin pathway during brain angiogenesis. *eLife* 4:e06489.
26. Ulrich F, et al. (2016) Reck enables cerebrovascular development by promoting canonical Wnt signaling. *Development* 143:147–159.
27. Chang J, et al. (2017) Gpr124 is essential for blood-brain barrier integrity in central nervous system disease. *Nat Med* 23:450–460.
28. Luhmann UF, et al. (2005) Role of the Norrie disease pseudoglioma gene in sprouting angiogenesis during development of the retinal vasculature. *Invest Ophthalmol Vis Sci* 46:3372–3382.
29. Vallon M, Essler M (2006) Proteolytically processed soluble tumor endothelial marker (TEM) 5 mediates endothelial cell survival during angiogenesis by linking integrin alpha(v)beta3 to glycosaminoglycans. *J Biol Chem* 281:34179–34188.
30. Vallon M, Rohde F, Janssen KP, Essler M (2010) Tumor endothelial marker 5 expression in endothelial cells during capillary morphogenesis is induced by the small GTPase Rac and mediates contact inhibition of cell proliferation. *Exp Cell Res* 316: 412–421.
31. Wang Y, Cho SG, Wu X, Siwko S, Liu M (2014) G-protein coupled receptor 124 (GPR124) in endothelial cells regulates vascular endothelial growth factor (VEGF)-induced tumor angiogenesis. *Curr Mol Med* 14:543–554.
32. Hernández-Vásquez MN, et al. (2017) Cell adhesion controlled by adhesion G protein-coupled receptor GPR124/ADGRA2 is mediated by a protein complex comprising intersectins and Elmo-Dock. *J Biol Chem* 292:12178–12191.
33. Oh J, et al. (2001) The membrane-anchored MMP inhibitor RECK is a key regulator of extracellular matrix integrity and angiogenesis. *Cell* 107:789–800.
34. Muraguchi T, et al. (2007) RECK modulates notch signaling during cortical neurogenesis by regulating ADAM10 activity. *Nat Neurosci* 10:838–845.
35. Ye X, Smallwood P, Nathans J (2011) Expression of the Norrie disease gene (Ndp) in developing and adult mouse eye, ear, and brain. *Gene Expr Patterns* 11:151–155.
36. Zhuo L, et al. (2001) hGFAP-cre transgenic mice for manipulation of glial and neuronal function in vivo. *Genesis* 31:85–94.
37. Liu H, Mohamed O, Dufort D, Wallace VA (2003) Characterization of Wnt signaling components and activation of the Wnt canonical pathway in the murine retina. *Dev Dyn* 227:323–334.
38. Van Raay TJ, Vetter ML (2004) Wnt/frizzled signaling during vertebrate retinal development. *Dev Neurosci* 26:352–358.
39. McNeill B, et al. (2012) Comparative genomics identification of a novel set of temporally regulated hedgehog target genes in the retina. *Mol Cell Neurosci* 49:333–340.
40. Robitaille J, et al. (2002) Mutant frizzled-4 disrupts retinal angiogenesis in familial exudative vitreoretinopathy. *Nat Genet* 32:326–330.
41. Jiao X, Ventruto V, Trese MT, Shastry BS, Hejtmancik JF (2004) Autosomal recessive familial exudative vitreoretinopathy is associated with mutations in LRP5. *Am J Hum Genet* 75:878–884.
42. Toomes C, et al. (2004a) Mutations in LRP5 or FZD4 underlie the common familial exudative vitreoretinopathy locus on chromosome 11q. *Am J Hum Genet* 74:721–730.
43. Toomes C, et al. (2004b) Spectrum and frequency of FZD4 mutations in familial exudative vitreoretinopathy. *Invest Ophthalmol Vis Sci* 45:2083–2090.
44. Ai M, Heeger S, Bartels CF, Schelling DK; Osteoporosis-Pseudoglioma Collaborative Group (2005) Clinical and molecular findings in osteoporosis-pseudoglioma syndrome. *Am J Hum Genet* 77:741–753.
45. Nikopoulos K, et al. (2010) Overview of the mutation spectrum in familial exudative vitreoretinopathy and Norrie disease with identification of 21 novel variants in FZD4, LRP5, and NDP. *Hum Mutat* 31:656–666.
46. Poulter JA, et al. (2010) Mutations in TSPAN12 cause autosomal-dominant familial exudative vitreoretinopathy. *Am J Hum Genet* 86:248–253.
47. Robitaille JM, et al. (2011) The role of frizzled-4 mutations in familial exudative vitreoretinopathy and Coats disease. *Br J Ophthalmol* 95:574–579.
48. Poulter JA, et al. (2012) Recessive mutations in TSPAN12 cause retinal dysplasia and severe familial exudative vitreoretinopathy (FEVR). *Invest Ophthalmol Vis Sci* 53: 2873–2879.
49. Panagiotou ES, et al. (2017) Defects in the cell signaling mediator β-catenin cause the retinal vascular condition FEVR. *Am J Hum Genet* 100:960–968.
50. Qin M, et al. (2005) Complexity of the genotype-phenotype correlation in familial exudative vitreoretinopathy with mutations in the LRP5 and/or FZD4 genes. *Hum Mutat* 26:104–112.
51. Kramer GD, Say EA, Shields CL (2016) Simultaneous novel mutations of LRP5 and TSPAN12 in a case of familial exudative vitreoretinopathy. *J Pediatr Ophthalmol Strabismus* 53 Online:e1–e5.
52. Khan AO, Lenzner S, Bolz HJ (2017) A family harboring homozygous FZD4 deletion supports the existence of recessive FZD4-related familial exudative vitreoretinopathy. *Ophthalmic Genet* 38:380–382.
53. Schatz P, Khan AO (2017) Variable familial exudative vitreoretinopathy in a family harbouring variants in both FZD4 and TSPAN12. *Acta Ophthalmol* 95:705–709.
54. Smith SE, Mullen TE, Graham D, Sims KB, Rehm HL (2012) Norrie disease: Extraocular clinical manifestations in 56 patients. *Am J Med Genet A* 158A:1909–1917.
55. Obermeier B, Daneman R, Ransohoff RM (2013) Development, maintenance and disruption of the blood-brain barrier. *Nat Med* 19:1584–1596.
56. Claxton S, et al. (2008) Efficient, inducible Cre-recombinase activation in vascular endothelium. *Genesis* 46:74–80.
57. Zhang C, et al. (2018) Endothelial cell–specific inactivation of TSPAN12 (tetraspanin 12) reveals pathological consequences of barrier defects in an otherwise intact vasculature. *Arterioscler Thromb Vasc Biol* 38:2691–2705.
58. Illing M, Molday LL, Molday RS (1997) The 220-kDa rim protein of retinal rod outer segments is a member of the ABC transporter superfamily. *J Biol Chem* 272: 10303–10310.
59. R Core Team (2013) R: A language and environment for statistical computing (R Foundation for Statistical Computing, Vienna). Available at www.R-project.org. Accessed June 29, 2018.